

Accepted Manuscript

Design and discovery of 2-(4-(1*H*-tetrazol-5-yl)-1*H*-pyrazol-1-yl)-4-(4-phenyl)thiazole derivatives as cardiotoxic agents via inhibition of PDE3

Li-Min Duan, Hong-Ying Yu, Yan-Long Li, Chun-Juan Jia

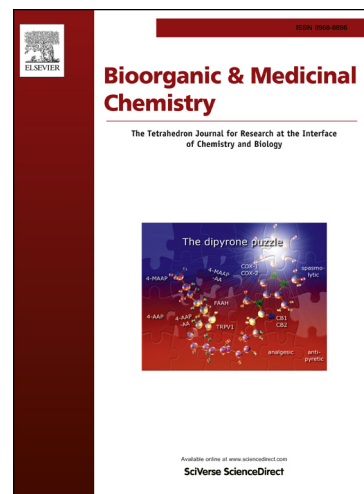
PII: S0968-0896(15)00669-0
DOI: <http://dx.doi.org/10.1016/j.bmc.2015.08.002>
Reference: BMC 12506

To appear in: *Bioorganic & Medicinal Chemistry*

Received Date: 2 July 2015
Revised Date: 1 August 2015
Accepted Date: 4 August 2015

Please cite this article as: Duan, L-M., Yu, H-Y., Li, Y-L., Jia, C-J., Design and discovery of 2-(4-(1*H*-tetrazol-5-yl)-1*H*-pyrazol-1-yl)-4-(4-phenyl)thiazole derivatives as cardiotoxic agents via inhibition of PDE3, *Bioorganic & Medicinal Chemistry* (2015), doi: <http://dx.doi.org/10.1016/j.bmc.2015.08.002>

This is a PDF file of an unedited manuscript that has been accepted for publication. As a service to our customers we are providing this early version of the manuscript. The manuscript will undergo copyediting, typesetting, and review of the resulting proof before it is published in its final form. Please note that during the production process errors may be discovered which could affect the content, and all legal disclaimers that apply to the journal pertain.





Design and discovery of 2-(4-(1*H*-tetrazol-5-yl)-1*H*-pyrazol-1-yl)-4-(4-phenyl)thiazole derivatives as cardiotoxic agents via inhibition of PDE3

Li-Min Duan^{a#}, Hong-Ying Yu^{b#*}, Yan-Long Li^c, Chun-Juan Jia^c

^a Department of Geriatric, DaQing Oil Field General Hospital, Da Qing, Heilongjiang 16300, China

^b Department of Cardiology, DaQing Oil Field General Hospital, Da Qing, Heilongjiang, 163001, China

^c Department of Internal Medicine, The People's Hospital of Shouguang, Shouguan, 262700, China

[#] Contributed equally to this work

ARTICLE INFO

Article history:

Received

Received in revised form

Accepted

Available online

Keywords:

Synthesis,
cardiotonic,
PDE3,
docking,
toxicity study

ABSTRACT

A series of novel 2-(4-(1*H*-tetrazol-5-yl)-1*H*-pyrazol-1-yl)-4-(4-phenyl)thiazole derivatives, 6(a-o) were designed, synthesized and evaluated for inhibitory activity against human PDE3A and PDE3B. In PDE3 assay, entire set of targeted analogues showed considerable inhibition of PDE3A ($IC_{50} = 0.24 \pm 0.06 - 16.42 \pm 0.14 \mu\text{M}$) over PDE3B ($IC_{50} = 2.34 \pm 0.13 - 28.02 \pm 0.03 \mu\text{M}$). Among the synthesized derivatives, compound 6d exhibited most potent inhibition of PDE3A with $IC_{50} = 0.24 \pm 0.06 \mu\text{M}$ than PDE3B ($IC_{50} = 2.34 \pm 0.13 \mu\text{M}$). This compound was further subjected for evaluation of cardiotoxic activity (contractile and chronotropic effects) in comparison with Vesnarinone. Results showed that, it selectively modulates the force of contraction ($63\% \pm 5$) rather than frequency rate ($23\% \pm 2$) at $100 \mu\text{M}$. Docking study of above compound was also carried out in the active site of PDE3 protein model to give proof to the mechanism of action of designed inhibitor. Further, in sub-acute toxicity experiment in Swiss-albino mice, it was found to be non-toxic up to 100 mg/kg dose for 28 days.

2009 Elsevier Ltd. All rights reserved.

1. Introduction

Cardiovascular diseases (CVDs) are considered as the foremost reason of death globally more than any other causes.¹ According to the recent estimates of WHO, 17.5 million people died from CVDs in 2012, representing 31% of all global deaths. Of these deaths, an estimated 7.4 million were due to coronary heart disease and 6.7 million were due to stroke.^{2,3,4} Alone in United States, about 5.1 million have congestive heart failure (CHF) which responsible for one in nine deaths in 2009. As a matter of fact, despite of advances in treatment, roughly half of the people who develop heart failure die within 5 years of diagnosis. It was also associated with economic burden which costs approximately \$32 billion each year in US, including cost of health care services, medications to treat heart failure, and missed days of work.^{5,6} Concerning to the sternness of the heart failures, novel and effective medication are need urgently.

For past few decades, glycosides obtained from digitalis have been used for the treatment of CHF. However, the clinical utility of these agents are seriously jeopardized due to their propensity to cause high life-threatening arrhythmias along with a low therapeutic index.^{7,8} These side effects could be overcome by using a novel class of 'non-glycoside' cardiotoxic agents which acts by selective inhibition of cyclic nucleotide phosphodiesterase (PDE) enzymes. These inhibitors offer better

Figure 1 Pharmacological significance of PDE3 Inhibitors.

safety profile and improved efficacy. The PDE enzymes are responsible for regulating the cellular levels of cyclic adenosine monophosphate (cAMP) and cyclic guanosine monophosphate (cGMP) by catalyzing the hydrolysis of these second messengers, fig 1.⁹ Based on the substrate specificity, kinetic properties, and

sensitivity to specific inhibitors, tissue distribution and sequence-derived information, 11 PDE families have been recognized in mammalian tissues. It includes PDE1, PDE2 to PDE11. Various PDEs, including PDE-3, are responsible for inducing vascular relaxation in different vascular beds when they are inhibited. Thus, inhibition of PDEs by specific inhibitors in cardiovascular tissues enhances cytosolic levels of cAMP which in turn causes a reduction in platelet aggregation, smooth muscle cell proliferation *in vitro*, and induction of a cardiotoxic effect. PDE3 was further sub-divided into two sub-types, viz., PDE3A and PDE3B, where, PDE3A is found in cardiac tissue, platelets and vascular smooth muscles, while PDE3B is prominently expressed in hepatocytes and adipose tissue. Therefore, selective inhibition of PDE3A offers acute inotropic and vasodilatory effects towards the treatment of CHF which warrant the discovery of new medication to this armamentarium of drugs.^{10,11}

Encouraged by the excellent phosphodiesterase activity of LQFM 021 (fig. 2), a novel pyrazole derivative,¹¹ present study deals with the synthesis of novel analogues of pyrazole tethered to other heterocyclic scaffolds i.e. tetrazole-pyrazole-thiazole conjugates. These constitutive compounds were evaluated for PDE3 inhibitory and cardiotoxic activity. Docking was also carried out to clarify the interaction of compounds with PDE3.

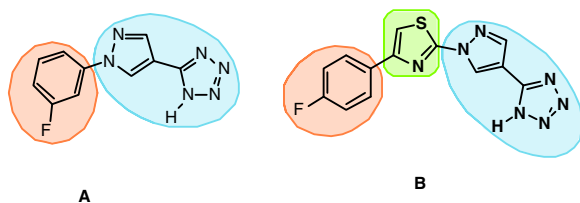


Figure 2 Structure of LQFM-021 (A) and designed inhibitor (B).

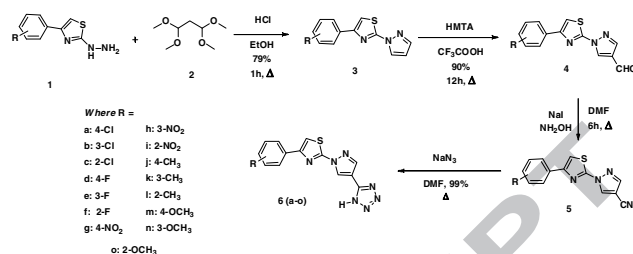
2.1. Results and discussion

2.1.1. Chemistry

The synthesis of title analogues was depicted in Scheme 1. Initially, the generation of target analogues begins with the synthesis of compound **3** in accordance with the method described by Finar and Godfrey.¹² Compound **3a** was then further subjected to Duff's Condition, where it selectively and regioselectively formylated to afford compound **4**.^{13,14,15} The synthesis of compound **5** was accomplished via the formation of the oxime of compound **4** in the presence of hydroxylamine. This was followed by *in situ* dehydration in the presence of sodium iodide and DMF at reflux temperature for 8 h to furnish **5**.¹⁶ The last step corresponds to the synthesis of compound (**6**) via 1,3-bipolar cycloaddition between compound **5** and sodium azide using ammonium chloride as the catalyst in DMF at reflux temperature for the period determined through TLC.

The FT-IR absorption bands of title compounds as presented in the experimental section showed a strong band at 3452-3498 cm^{-1} which is attributed to primary N-H stretching frequency. The presence of C=N group was confirmed at 1628-1678 cm^{-1} . Moreover, the occurrence of strong band at 2956-2982 cm^{-1} showed the stretching frequencies of Ar C-H group, whereas the presence of Cl on phenyl ring was observed at 1092-887 cm^{-1} . The C-N group was observed at 1208-1268 cm^{-1} . Title compounds showed another band at 681-693 cm^{-1} corresponding to C-S-C stretching vibration. The ¹H-NMR spectra showed the resonance of Ar-H in the range of 8.01 to 7.45 ppm. The presence of protons of N-H groups is confirmed via singlet at 3.59-3.58

ppm, whereas resonance of pyrazole protons found as a singlet in the region 8.93-8.89 ppm along with another singlet at 8.40-8.42 ppm for proton of thiazole ring. Finally all the structure of title compounds was established by mass and elemental analysis.



Scheme 1 Synthetic Route for the Preparation of 2-(4-(1H-tetrazol-5-yl)-1H-pyrazol-1-yl)-4-substituted phenylthiazole **6**(a-o).

2.1.2. Pharmacological Activity

The synthesized target compounds were assessed for their PDE3 (types A and B) inhibitory activities in comparison with Vesnarinone and the results were shown in Table 1.

Table 1: Enzyme inhibitory assessment data of compounds **5** (a-o) and Vesnarinone.

Compound	IC ₅₀ (in μM)	
	PDE3A	PDE3B
6a	2.45 ± 0.13	3.83 ± 0.06
6b	2.99 ± 0.05	5.01 ± 0.02
6c	3.62 ± 0.08	5.92 ± 0.05
6d	0.24 ± 0.06	2.34 ± 0.13
6e	1.45 ± 0.12	4.65 ± 0.04
6f	1.89 ± 0.06	4.72 ± 0.11
6g	6.23 ± 0.04	7.27 ± 0.07
6h	6.89 ± 0.05	8.54 ± 0.02
6i	7.43 ± 0.11	10.21 ± 0.05
6j	8.15 ± 0.07	16.72 ± 0.03
6k	9.12 ± 0.08	14.49 ± 0.15
6l	9.89 ± 0.06	16.62 ± 0.01
6m	13.44 ± 0.02	25.62 ± 0.07
6n	14.63 ± 0.03	25.11 ± 0.05
6o	16.42 ± 0.14	28.02 ± 0.03
Vesnarinone	11.21 ± 0.05	14.54 ± 0.03

Among the synthesized compounds, **6d** was disclosed as the most potent inhibitor for both PDE3A (0.24 ± 0.06 μM) and PDE3B (2.34 ± 0.13 μM). While changing the pattern of the substitution of fluoro group leads to prominently decline in activity against PDE3B and less against PDE3A. Against PDE3B, the introduction of chloro group at the *para* position (**6a**), showed considerable decline in potency and this was followed by other analogues having isomeric replacements. While against the PDE3A, these compounds showed marginally improved IC₅₀ values. Furthermore, marked decline in inhibitory activity was reported by compounds **6g**, **6h** and **6i** having isomeric substitution of nitro group, where they significantly inhibit PDE3A than PDE3B. It is noteworthy to mention that, introduction of electron donating substituent, renders compounds least active and even some cases found less potent than Vesnarinone as standard. For instance, compound **6j**, **6k** and **6l**, against PDE3A, showed IC₅₀ values ranging from (8.15 ± 0.07 - 9.89 ± 0.06 μM). The same inhibition pattern for these compounds was observed against PDE3B, but with less potency, except compound **6k**, which found almost equipotent to Vesnarinone. Rest of the compounds, viz., **6m** (13.44 ± 0.02 μM),

6n ($14.63 \pm 0.03 \mu\text{M}$) and 6o ($16.42 \pm 0.14 \mu\text{M}$) showed reduced activity in comparison to standard ($11.21 \pm 0.05 \mu\text{M}$). In PDE3B inhibition assay, these compounds found almost ten-to-fourteen folds less potent than standard. From the results, it was indicated that, the inhibition potency of the compounds will follow a comprehensible structural pattern. Results showed that, compounds containing electron withdrawing substituent found more potent than electron donating and *para* is the most favourable position of substituent than *ortho* and *meta*. Thus, the structural-activity relationships of these inhibitors have been shown in Fig 3.

Figure 3 SAR of the compounds 6 (a-o)

Due to over expression of PDE3A in cardiac tissues than PDE3B, compound 6d which had showed the best PDE3A inhibitory activity was tested for its effect on the force of contraction and frequency rate. For this experiment, spontaneously beating atria of rat was taken in comparison with vesnarinone. To avoid the interference of catecholamine release, reserpine-pretreated animals were used in the study. Results showed that, it increases the cardiac contractility more efficiently ($63\% \pm 5$) than Vesnarinone ($50\% \pm 4$) at $100 \mu\text{M}$. After washing of the myocardial preparations, the atria of the subject have regained the contractility to the pre-drug state. This behaviour suggests that, the action of compound 6d is reversible and original state could be achieved after removing the drug. On the other hand, it does not considerably enhance the force of the contraction ($23\% \pm 2$) in comparison to Standard ($21\% \pm 7$). This enables us to understand that, it act as inotropic agent without causing significant arrhythmias, Table 2.

Table 2: Effects of the compound 6d on force of contractility and frequency rate.#

Parameter	Compound	Base	1×10^{-6}	1×10^{-5}	1×10^{-4}
Contractile force	6d	100 ± 4	110 ± 6	129 ± 3	163 ± 5
	Vesnarinone	100 ± 2	105 ± 4	125 ± 3	150 ± 4
Frequency Rate	6d	100 ± 3	108 ± 4	114 ± 4	123 ± 2
	Vesnarinone	100 ± 5	105 ± 3	112 ± 2	121 ± 7

The effect of each concentration (mol L^{-1}) of a compound was defined by the difference between the contraction and frequency before and after its addition to the bathing fluid, and was expressed as a percent variation in contraction and frequency in respect to the controls. Results are means \pm SEM from six atria.

With in vitro results in hand, docking study of most active compound 6d was carried out in the active site of PDE3 protein model to give proof to the mechanism of action of designed inhibitor. Docking was conducted with the CDOCKER program in Discovery Studio 2.5 (Accelrys, San Diego, USA). This study

was conducted to define the orientation and interaction of 6d with PDE3. For this study, catalytic domain of human phosphodiesterase 3b in complex with a dihydropyridazine inhibitor (ISO2) was downloaded from protein data bank and heteroatoms including the water molecules were cleaned (clean geometry) using Discovery Studio. It was selected due to reasonable homology between PDE3A and PDE3B, where their identities and positives were obtained as 48% and 67%, respectively, extracted from NCBI-BLAST.^{17, 18, 19} This homology was further increased to approximately 95% within 15Å region in and around active site.^{20, 21} The ligand 6d was docked in the active site defined over the co-crystallised dihydropyridazine inhibitor with the help of Binding-Site module within the Discovery studio 2.5.

On the whole, CDOCKER is a grid-based molecular docking method that employs CHARMM force fields. This protein was firstly held rigid while the ligand was allowed to freely rotate during the refinement. Two hundred random ligand conformations were then generated from the initial ligand structure through high temperature molecular dynamics, followed by random rotations; refinement by grid-based (GRID 1) simulated annealing, and a final grid-based or full force field minimisation. In this experiment, the ligand was heated to a temperature of 700 K in 2000 steps. The cooling steps were set to 5000 steps with 300 K cooling temperature. The grid extension was set to 10 Å. Hydrogen atoms were added to the structure and all ionisable residues were set at their default protonation state at a neutral pH. For ligand 6d, ten ligand binding poses were ranked according to their CDOCKER energies, and the predicted binding interactions were analysed. Furthermore, best among the ten ligand binding pose was chosen and carried out in-situ ligand minimization using standard protocol.

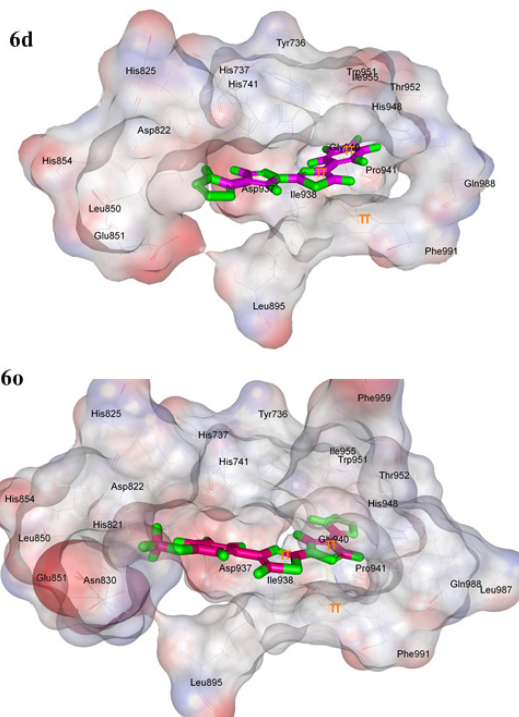


Figure 4 Three dimensional schematic representation of the ligand 6d (most active) and 6o (least active) with that of human phosphodiesterase 3b.

Results revealed that, 6d was efficiently buried and engulfed in the active site of PDE3 by making close interatomic contacts. It was found that tetrazole-pyrazole portion of compound 6d was surrounded by His731, His737, His825 and Asp822, fig. 4. The formation of one hydrogen bond with Asp822 with tetrazole ring of the ligand was also revealed which depicts its better affinity against the target protein. It was also revealed that, channelling of thiazole and its neighbouring phenyl fragment deep inside the pocket lined with residues like Tyr737, Phe559 and Phe991 would contribute to enhanced affinity and better stabilisation of compound 6d within the active site. Inside the deep cleft of the active site, compound 6d showed the formation of two non-covalent pi-pi stacking interaction between engulfed aromatic residues of the ligand with Phe991, a key catalytic amino acid residue of PDE3. On the contrary, the orientation of the ligand was found different in the case of least active compound 6o. As shown in figure 4, it showed the formation of two pi-pi interaction with Phe991 along with one H-bond with Thr952. However the tetrazole ring was found oriented in deep cleft of the active site in opposite manner to that of compound 6d. On comparing both ligand (6d and 6o), the engulfment of phenyl thiazole in deeper cleft lined by Gly940, Pro941, His948, Gln988 and Thr952 serve as vital factor for the generation of activity, while distortion from this orientation render compound non active, i.e., compound 6o.

The docked interaction of LQFM-021 was found similar to the docked complex of most promising inhibitor 6d, we found that both ligand shares a common interaction with Phe991, a key catalytic residue. Moreover, the aromatic portion of the molecules was found protruded towards the inner cleft lined by His737, His741, His948, Thr952, Gln988, Gly940, Pro941 and Thr952.

Earlier studies suggests that, similar interaction was observed in the case of other various PDE3A inhibitors, including Vesnarinone, which suggests that, our designed molecules could be act in similar fashion.

To confirm the potential application of compound 6d as viable lead for drug development, it should possess no toxicity along with potent bioactivity. After establishing pharmacological activity of compound 6d, it's worthwhile to perform its toxicity evaluation. Thus, in acute toxicity study, it has been found to be safe upto 1000 mg/kg as a single acute oral dose. Hence, sub acute experiment was conducted in accordance with the Organization for Economic Co-operation and Development (OECD) test guideline No 423, and the same has been illustrated in experimental section.

There were no observational changes; morbidity and mortality found in experimental animals throughout the period up to 28 days at the dose level of 100 mg/kg body weight, once orally. The blood and serum samples upon analysis showed no major changes in total haemoglobin level, RBC count, WBC count, SGOT, creatinine, triglycerides, cholesterol, albumin (Table 3). On the basis of gross pathological study of animals, no changes in any of the organs studied including their absolute and relative weight were found. Hence, the experiment showed that compound 6d is well tolerated by the Swiss albino mice up to the dose level of 100 mg/kg body weight once orally for 28 days in sub-acute toxicity study.

Table 3: Effect of compound 6d at 0.1, 1, 10 and 100 mg/kg body weight once orally for 28 days in sub acute toxicity study on body weight, haematological and serum biochemical

parameters in Swiss albino mice (Mean \pm SD; n = 6; and P < 0.05 compared to control, 0.1, 1, 10 and 100 mg/kg).

Parameter	Dose in mg/kg body weight once orally for 28 days				
	Control	0.1	1	10	100
Body Weight	31.2 \pm 1.6	29.28 \pm 2.1	28.04 \pm 1.7	32.62 \pm 3.2	33.0 \pm 4.5
RBC (x 10/mm ³)	7.2 \pm 1.1	7.13 \pm 0.8	7.47 \pm 1.3	7.83 \pm 0.8	7.74 \pm 0.5
WBC (x 10/mm ³)	6.1 \pm 1.3	6.91 \pm 2.6	5.41 \pm 0.7	5.68 \pm 3.1	6.9 \pm 0.2
Haemoglobin (g/dL)	13.87 \pm 0.46	14.5 \pm 0.2	15.34 \pm 0.45	15.72 \pm 0.01	15.24 \pm 1.34
Cholesterol (mg/dL)	138.43 \pm 1.52	125.66 \pm 1.30	129.03 \pm 2.56	135.4 \pm 2.04	134.3 \pm 0.34
Triglycerides (mg/dL)	263.69 \pm 3.38	254.1 \pm 4.61	247.26 \pm 2.89	251.86 \pm 2.15	255.4 \pm 0.22
Total Protein (mg/dL)	3.45 \pm 0.45	3.96 \pm 1.12	3.64 \pm 0.11	4.12 \pm 0.45	4.54 \pm 0.36
Creatinine (mg/dL)	0.04 \pm 0.37	0.04 \pm 0.07	0.04 \pm 0.02	0.04 \pm 0.45	0.05 \pm 3.5
ALP (U/L)	132.4 \pm 6.26	135.5 \pm 3.4	136.6 \pm 0.5	133.3 \pm 8.9	134.02 \pm 4.6
Albumin (g/dL)	2.78 \pm 1.82	2.89 \pm 0.01	2.61 \pm 0.03	2.57 \pm 0.05	2.59 \pm 2.3
SGPT (U/L)	41.46 \pm 17.25	40.12 \pm 13.34	41.34 \pm 0.03	41.8 \pm 2.7	42.1 \pm 4.3
SGOT (U/L)	112.7 \pm 10.6	107.8 \pm 6.78	109.8 \pm 8.45	110.2 \pm 12.67	111.6 \pm 12.31

3. Conclusions

In conclusion, we have efficiently synthesized 2-(4-(1H-tetrazol-5-yl)-1H-pyrazol-1-yl)-4-substituted phenylthiazole **6(a-o)** as cardiotoxic agents in good yields. It has been found that, minor structural variation render compound active. SAR studies suggest that, compounds containing electron withdrawing substituent found more potent than electron donating and among them *para* is the most favourable position of substituent than *ortho* and *meta*. Together with selective and potent inhibition of PDE3A along with efficient inotropic action, compound 6d could be act as a lead for the future drug discovery against CHF.

4. Experimental

4.1. Animals, drugs, chemicals and instruments

Adult male Wistar rats (250–350 g), were kept in controlled environmental conditions (temperature: 23 \pm 2 °C; light-dark cycle: 7 am to 7 pm) and had a free access to a standard laboratory diet and water. In order to obtain atrial preparation, depleted in endogenous catecholamine, the animals were treated intraperitoneally with reserpine (5 mg/kg b.wt) 24 h before euthanasia.¹⁰ In each experiment, the animals were anaesthetized with intraperitoneal injection of thiopental 80 mg/kg, and after midline thoracotomy, the heart was rapidly excised and placed in a dissection dish filled with oxygenated Krebs-Henseleit

solution. The enzymes were obtained from BPS BioScience Inc. All chemicals purchased from Merck and Fluka Chemical Co. The experiments were performed in compliance with Institutional Animal Ethical Committee of DaQing Oil Field General Hospital, China.

All chemicals were of analytical grade and used directly. Melting points were determined in open capillary tubes with electrothermal melting point apparatus (MP-1) and are uncorrected. The completion of reaction was checked by thin layer chromatography (TLC) using silica gel-G coated Al-plates (0.5 mm thickness, Merck; Solvent system: benzene:ethyl acetate) and the plates were illuminated under UV (254 nm) and evaluated in iodine vapor. The solubility of all the compounds were tested by using water, chloroform, ethanol, DMF, DMSO, benzene, acetic acid, ethyl acetate, and dilute acids. FT-IR (in 2.0 cm⁻¹, flat, smooth, abex, KBr) spectra were recorded on Perkin Elmer-Spectrum RX-I spectrometer. Elemental analysis was carried out on a Vario EL III CHNOS elementor analyzer. ¹H NMR spectra were recorded on a Bruker Avance II 400 NMR Spectrometer and the ¹³C NMR spectra on a Bruker Avance II 100 NMR spectrometer in DMSO-d₆ using TMS as the internal standard. The chemical shifts are reported in parts per million (ppm, d), and signals are described as s (singlet), d (doublet), t (triplet), q (quartet), and m (multiplet). Mass spectra were obtained on VG-AUTOSPEC spectrometer. The developed tension was recorded isometrically by means of a high-sensitivity force transducer (type E, Zimmermann, Eipzig-Berlin) connected to powerlab 8/30 (model 870). Solvents were purified prior to use according to standard procedure.

4.2.1. Synthesis of 2-(4-(1H-tetrazol-5-yl)-1H-pyrazol-1-yl)-4-sustituted phenylthiazole 6(a-o)

A mixture of 1-(substituted phenylthiazol-2-yl)-1H-pyrazole-4-carbonitrile (**5**) (10 mmol), sodium azide (60 mmol), and ammonium chloride (60 mmol) in 40 mL of DMF was heated at reflux temperature for 72 h. The completion of the reaction has been assessed using the TLC using the different polarity of the solvents. The resultant reaction mixture was then poured into water and acidified to pH 5. The product was vacuum filtered and dried to provide compound **6**.

4.2.1.1. 2-(4-(1H-tetrazol-5-yl)-1H-pyrazol-1-yl)-4-(4-chlorophenyl)thiazole (6a)

White-crystals; Yield: 72%; M.p: 189-191 °C; MW: 329.77; R_f: 0.64; FT-IR (ν_{max}; cm⁻¹ KBr): 3452 (N-H stretch), 3028, 2956 (C-H stretch), 1628 (C=N stretch), 1208 (C-N stretch), 1193 (C-S), 1092 (aromatic-Cl), 762, 693 (C-S-C) cm⁻¹; ¹H-NMR (400MHz, CDCl₃, TMS) δ ppm: 8.93 (d, 1H J =1.88 Hz, pyrazol), 8.40 (s, 1H thiazole), 8.26 (d, 1H J =1.81 Hz, pyrazol), 7.95–7.93 (m, 2H,Ar-H), 7.53-7.51 (m, 2H,Ar-H), 3.59 (br-s, 1H, tetrazol, NH); ¹³C-NMR (100MHz, CDCl₃) δ,ppm: 163.5, 158.5, 149.9, 137.6, 134.2, 131.9, 129.6, 129.1, 128.9, 108.5, 102.3; Mass : 330.79 (M+1); Elemental analysis for C₁₃H₈ClN₇S: Calculated: C, 47.35; H, 2.45; N, 29.73; Found: C, 47.38; H, 2.45; N, 29.76.

4.2.1.2. 2-(4-(1H-tetrazol-5-yl)-1H-pyrazol-1-yl)-4-(3-chlorophenyl)thiazole. (6b)

White-crystals; Yield: 68%; M.p: 206-208 °C; MW: 329.77; R_f: 0.71; FT-IR (ν_{max}; cm⁻¹ KBr): 3458 (N-H stretch), 3035, 2968 (C-H stretch), 1642 (C=N stretch), 1210 (C-N stretch), 1196 (C-S), 887 (aromatic-Cl), 768, 681 (C-S-C) cm⁻¹; ¹H-NMR (400MHz,

CDCl₃, TMS) δ ppm: 8.95 (d, 1H J =1.84 Hz, pyrazol), 8.45 (s, 1H thiazole), 8.19 (d, 1H J =1.71 Hz, pyrazol), 8.01–7.98 (m, 2H,Ar-H), 7.45-747 (m, 2H,Ar-H), 3.51 (br-s, 1H, tetrazol, NH); ¹³C-NMR (100MHz, CDCl₃) δ,ppm: 163.4, 157.5, 149.8, 137.6, 134.9, 134.4, 129.6, 129.4, 129.2, 128.8, 125.7, 108.5, 102.3; Mass : 330.79 (M+1); Elemental analysis for C₁₃H₈ClN₇S: Calculated: C, 47.35; H, 2.45; N, 29.73; Found: C, 47.34; H, 2.48; N, 29.75.

4.2.1.3. 2-(4-(1H-tetrazol-5-yl)-1H-pyrazol-1-yl)-4-(2-chlorophenyl)thiazole. (6c)

White yellow-crystals; Yield: 78%; M.p: 216-218 °C; MW: 329.77; R_f: 0.62; FT-IR (ν_{max}; cm⁻¹ KBr): 3462 (N-H stretch), 3047, 2961 (C-H stretch), 1649 (C=N stretch), 1215 (C-N stretch), 1185 (C-S), 872 (aromatic-Cl), 756, 685 (C-S-C) cm⁻¹; ¹H-NMR (400MHz, CDCl₃, TMS) δ ppm: 8.89 (d, 1H J =1.79 Hz, pyrazol), 8.42 (s, 1H thiazole), 8.23 (d, 1H J =1.75 Hz, pyrazol), 7.73–7.62 (m, 2H,Ar-H), 7.39-736 (m, 2H,Ar-H), 3.58 (br-s, 1H, tetrazol, NH); ¹³C-NMR (100MHz, CDCl₃) δ,ppm: 163.6, 158.4, 152.3, 137.6, 132.5, 132.2, 130.9, 130.2, 129.6, 129.2, 128.9, 108.6, 102.3; Mass : 330.79 (M+1); Elemental analysis for C₁₃H₈ClN₇S: Calculated: C, 47.35; H, 2.45; N, 29.73; Found: C, 47.38; H, 2.43; N, 29.78.

4.2.1.4. 2-(4-(1H-tetrazol-5-yl)-1H-pyrazol-1-yl)-4-(4-fluorophenyl)thiazole. (6d)

Brown-crystals; Yield: 62%; M.p: 198-201 °C; MW: 313.31; R_f: 0.58; FT-IR (ν_{max}; cm⁻¹ KBr): 3472 (N-H stretch), 3058, 2968 (C-H stretch), 1642 (C=N stretch), 1225 (C-N stretch), 1187 (C-S), 863 (aromatic-F), 758, 682 (C-S-C) cm⁻¹; ¹H-NMR (400MHz, CDCl₃, TMS) δ ppm: 8.87 (d, 1H J =1.68 Hz, pyrazol), 8.56 (s, 1H thiazole), 8.25 (d, 1H J =1.78 Hz, pyrazol), 7.64–7.61 (m, 2H,Ar-H), 7.25-721 (m, 2H,Ar-H), 3.64 (br-s, 1H, tetrazol, NH); ¹³C-NMR (100MHz, CDCl₃) δ,ppm: 163.4, 162.8, 158.5, 149.6, 137.3, 130.7, 129.4, 128.6, 116.2, 108.7, 102.4; Mass : 314.38 (M+1); Elemental analysis for C₁₃H₈FN₇S: Calculated: C, 49.83; H, 2.57; N, 31.29; Found: C, 49.85; H, 2.57; N, 31.28.

4.2.1.5. 2-(4-(1H-tetrazol-5-yl)-1H-pyrazol-1-yl)-4-(3-fluorophenyl)thiazole. (6e)

Light brown-crystals; Yield: 73%; M.p: 208-211 °C; MW: 313.31; R_f: 0.69; FT-IR (ν_{max}; cm⁻¹ KBr): 3478 (N-H stretch), 3064, 2976 (C-H stretch), 1648 (C=N stretch), 1228 (C-N stretch), 1192 (C-S), 868 (aromatic-F), 762, 676 (C-S-C) cm⁻¹; ¹H-NMR (400MHz, CDCl₃, TMS) δ ppm: 8.83 (d, 1H J =1.82 Hz, pyrazol), 8.48 (s, 1H thiazole), 8.23 (d, 1H J =1.74 Hz, pyrazol), 7.58–7.54 (m, 2H,Ar-H), 7.21-718 (m, 2H,Ar-H), 3.56 (br-s, 1H, tetrazol, NH); ¹³C-NMR (100MHz, CDCl₃) δ,ppm: 163.7, 162.1, 158.2, 149.9, 137.6, 134.7, 129.2, 127.4, 123.3, 115.9, 115.2, 108.3, 102.7; Mass : 314.38 (M+1); Elemental analysis for C₁₃H₈FN₇S: Calculated: C, 49.83; H, 2.57; N, 31.29; Found: C, 49.87; H, 2.59; N, 31.32.

4.2.1.6. 2-(4-(1H-tetrazol-5-yl)-1H-pyrazol-1-yl)-4-(2-fluorophenyl)thiazole. (6f)

Brown-crystals; Yield: 58%; M.p: 203-205 °C; MW: 313.31; R_f: 0.62; FT-IR (ν_{max}; cm⁻¹ KBr): 3484 (N-H stretch), 3052, 2979 (C-H stretch), 1651 (C=N stretch), 1239 (C-N stretch), 1198 (C-S), 862 (aromatic-F), 768, 669 (C-S-C) cm⁻¹; ¹H-NMR (400MHz, CDCl₃,

TMS) δ ppm: 8.87 (d, 1H J =1.85 Hz, pyrazol), 8.45 (s, 1H thiazole), 8.21 (d, 1H J =1.72 Hz, pyrazol), 7.53–7.51 (m, 2H,Ar-H), 7.18-716 (m, 2H,Ar-H), 3.52 (br-s, 1H, tetrazol, NH); ^{13}C -NMR (100MHz, CDCl_3) δ ,ppm: 163.4, 158.5, 157.9, 152.6, 137.8, 130.9, 129.5, 128.8, 124.8, 123.5, 114.7, 108.5, 102.4; Mass : 314.38 (M+1); Elemental analysis for $\text{C}_{13}\text{H}_8\text{FN}_7\text{S}$: Calculated: C, 49.83; H, 2.57; N, 31.29; Found: C, 49.84; H, 2.57; N, 31.27.

4.2.1.7. 2-(4-(1H-tetrazol-5-yl)-1H-pyrazol-1-yl)-4-(4-nitrophenyl)thiazole. (6g)

Yellow-crystals; Yield: 69%; M.p: 223-225 °C; MW: 340.32; R_f : 0.75; FT-IR (ν_{max} ; cm^{-1} KBr): 3476 (N-H stretch), 3054, 2972 (C-H stretch), 1659 (C=N stretch), 1358 (NO stretch), 1242 (C-N stretch), 1189 (C-S), 784, 679 (C-S-C) cm^{-1} ; ^1H -NMR (400MHz, CDCl_3 , TMS) δ ppm: 8.78 (d, 1H J =1.73 Hz, pyrazol), 8.42 (s, 1H thiazole), 8.14 (d, 1H J =1.63 Hz, pyrazol), 7.78–7.73 (m, 2H,Ar-H), 7.24-722 (m, 2H,Ar-H), 3.62 (br-s, 1H, tetrazol, NH); ^{13}C -NMR (100MHz, CDCl_3) δ ,ppm: 163.7, 158.2, 149.7, 147.2, 139.1, 137.5, 129.2, 126.3, 124.4, 108.1, 102.5; Mass : 341.34 (M+1); Elemental analysis for $\text{C}_{13}\text{H}_8\text{N}_8\text{O}_2\text{S}$: Calculated: C, 45.88; H, 2.37; N, 32.93; Found: C, 45.89; H, 2.36; N, 32.93.

4.2.1.8. 2-(4-(1H-tetrazol-5-yl)-1H-pyrazol-1-yl)-4-(3-nitrophenyl)thiazole. (6h)

Light yellow-crystals; Yield: 73%; M.p: 216-218 °C; MW: 340.32; R_f : 0.53; FT-IR (ν_{max} ; cm^{-1} KBr): 3484 (N-H stretch), 3057, 2971 (C-H stretch), 1654 (C=N stretch), 1359 (NO stretch), 1248 (C-N stretch), 1193 (C-S), 789, 682 (C-S-C) cm^{-1} ; ^1H -NMR (400MHz, CDCl_3 , TMS) δ ppm: 8.94 (d, 1H J =1.68 Hz, pyrazol), 8.38 (s, 1H thiazole), 8.32 (d, 1H J =1.59 Hz, pyrazol), 7.96–7.93 (m, 2H,Ar-H), 7.14-712 (m, 2H,Ar-H), 3.57 (br-s, 1H, tetrazol, NH); ^{13}C -NMR (100MHz, CDCl_3) δ ,ppm: 163.3, 158.5, 149.9, 148.4, 137.6, 133.9, 132.9, 130.6, 129.2, 123.9, 122.7, 108.3, 102.4; Mass : 341.38 (M+1); Elemental analysis for $\text{C}_{13}\text{H}_8\text{N}_8\text{O}_2\text{S}$: Calculated: C, 45.88; H, 2.37; N, 32.93; Found: C, 45.87; H, 2.37; N, 32.95.

4.2.1.9. 2-(4-(1H-tetrazol-5-yl)-1H-pyrazol-1-yl)-4-(2-nitrophenyl)thiazole. (6i)

Yellow-crystals; Yield: 62%; M.p: 232-235 °C; MW: 340.32; R_f : 0.48; FT-IR (ν_{max} ; cm^{-1} KBr): 3489 (N-H stretch), 3052, 2974 (C-H stretch), 1658 (C=N stretch), 1362 (NO stretch), 1256 (C-N stretch), 1198 (C-S), 795, 686 (C-S-C) cm^{-1} ; ^1H -NMR (400MHz, CDCl_3 , TMS) δ ppm: 8.93 (d, 1H J =1.69 Hz, pyrazol), 8.18 (s, 1H thiazole), 8.33 (d, 1H J =1.62 Hz, pyrazol), 7.94–7.93 (m, 2H,Ar-H), 7.21-723 (m, 2H,Ar-H), 3.54 (br-s, 1H, tetrazol, NH); ^{13}C -NMR (100MHz, CDCl_3) δ ,ppm: 163.7, 158.2, 152.5, 148.8, 137.5, 135.3, 132.6, 129.6, 128.9, 125.2, 124.4, 108.7, 102.3; Mass: 341.32 (M+1); Elemental analysis for $\text{C}_{13}\text{H}_8\text{N}_8\text{O}_2\text{S}$: Calculated: C, 45.88; H, 2.37; N, 32.93; Found: C, 45.88; H, 2.39; N, 32.92.

4.2.1.10. 2-(4-(1H-tetrazol-5-yl)-1H-pyrazol-1-yl)-4-(p-tolyl)thiazole. (6j)

Brown-crystals; Yield: 75%; M.p: 195-197 °C; MW: 309.35; R_f : 0.52; FT-IR (ν_{max} ; cm^{-1} KBr): 3482 (N-H stretch), 3058, 2976 (C-H stretch), 2946 (CH_3), 1664 (C=N stretch), 1252 (C-N stretch), 1189 (C-S), 792, 684 (C-S-C) cm^{-1} ; ^1H -NMR (400MHz, CDCl_3 , TMS)

δ ppm: 8.95 (d, 1H J =1.72 Hz, pyrazol), 8.21 (s, 1H thiazole), 8.38 (d, 1H J =1.68 Hz, pyrazol), 7.53–7.49 (m, 2H,Ar-H), 7.22-721 (m, 2H,Ar-H), 3.52 (br-s, 1H, tetrazol, NH), 2.27 (s, 3H, CH_3); ^{13}C -NMR (100MHz, CDCl_3) δ ,ppm: 163.2, 158.7, 149.8, 137.6, 131.7, 130.2, 129.5, 128.8, 125.7, 108.5, 102.4, 21.3; Mass: 310.32 (M+1); Elemental analysis for $\text{C}_{14}\text{H}_{11}\text{N}_7\text{S}$: Calculated: C, 54.36; H, 3.58; N, 31.69; Found: C, 54.37; H, 3.59; N, 31.71.

4.2.1.11. 2-(4-(1H-tetrazol-5-yl)-1H-pyrazol-1-yl)-4-(m-tolyl)thiazole. (6k)

Light brown-crystals; Yield: 71%; M.p: 213-214 °C; MW: 309.35; R_f : 0.59; FT-IR (ν_{max} ; cm^{-1} KBr): 3492 (N-H stretch), 3068, 2982 (C-H stretch), 2953 (CH_3), 1672 (C=N stretch), 1258 (C-N stretch), 1182 (C-S), 785, 682 (C-S-C) cm^{-1} ; ^1H -NMR (400MHz, CDCl_3 , TMS) δ ppm: 8.92 (d, 1H J =1.71 Hz, pyrazol), 8.26 (s, 1H thiazole), 8.32 (d, 1H J =1.58 Hz, pyrazol), 7.75–7.73 (m, 2H,Ar-H), 7.28-724 (m, 2H,Ar-H), 3.57 (br-s, 1H, tetrazol, NH), 2.34 (s, 3H, CH_3); ^{13}C -NMR (100MHz, CDCl_3) δ ,ppm: 163.3, 158.3, 149.8, 138.9, 137.6, 132.9, 130.4, 129.1, 129.0, 128.9, 124.5, 108.5, 102.3, 21.6; Mass: 310.39 (M+1); Elemental analysis for $\text{C}_{14}\text{H}_{11}\text{N}_7\text{S}$: Calculated: C, 54.36; H, 3.58; N, 31.69; Found: C, 54.39; H, 3.61; N, 31.68.

4.2.1.12. 2-(4-(1H-tetrazol-5-yl)-1H-pyrazol-1-yl)-4-(o-tolyl)thiazole. (6l)

Dark brown-crystals; Yield: 78%; M.p: 221-224 °C; MW: 309.35; R_f : 0.63; FT-IR (ν_{max} ; cm^{-1} KBr): 3498 (N-H stretch), 3074, 2978 (C-H stretch), 2959 (CH_3), 1676 (C=N stretch), 1262 (C-N stretch), 1188 (C-S), 789, 687 (C-S-C) cm^{-1} ; ^1H -NMR (400MHz, CDCl_3 , TMS) δ ppm: 8.95 (d, 1H J =1.92 Hz, pyrazol), 8.22 (s, 1H thiazole), 8.38 (d, 1H J =1.57 Hz, pyrazol), 7.54–7.52 (m, 2H,Ar-H), 7.32-728 (m, 2H,Ar-H), 3.51 (br-s, 1H, tetrazol, NH), 2.18 (s, 3H, CH_3); ^{13}C -NMR (100MHz, CDCl_3) δ ,ppm: 163.2, 158.3, 152.3, 137.4, 136.9, 129.7, 129.5, 129.1, 128.6, 126.2, 122.7, 108.1, 102.3, 18.7; Mass: 310.31 (M+1); Elemental analysis for $\text{C}_{14}\text{H}_{11}\text{N}_7\text{S}$: Calculated: C, 54.36; H, 3.58; N, 31.69; Found: C, 54.37; H, 3.56; N, 31.72.

4.2.1.13. 2-(4-(1H-tetrazol-5-yl)-1H-pyrazol-1-yl)-4-(4-methoxyphenyl)thiazole. (6m)

Dark green-crystals; Yield: 58%; M.p: 235-237 °C; MW: 325.35; R_f : 0.73; FT-IR (ν_{max} ; cm^{-1} KBr): 3482 (N-H stretch), 3079, 2975 (C-H stretch), 1672 (C=N stretch), 1668 (C-O stretch), 1268 (C-N stretch), 1197 (C-S), 782, 681 (C-S-C) cm^{-1} ; ^1H -NMR (400MHz, CDCl_3 , TMS) δ ppm: 8.92 (d, 1H J =1.86 Hz, pyrazol), 8.12 (s, 1H thiazole), 8.24 (d, 1H J =1.52 Hz, pyrazol), 7.51–7.50 (m, 2H,Ar-H), 7.02-703 (m, 2H,Ar-H), 3.73 (s, 3H, OCH_3), 3.48 (br-s, 1H, tetrazol, NH); ^{13}C -NMR (100MHz, CDCl_3) δ ,ppm: 163.4, 160.6, 158.5, 149.9, 137.2, 129.3, 128.3, 125.7, 114.8, 108.5, 102.3, 55.2; Mass: 326.37 (M+1); Elemental analysis for $\text{C}_{14}\text{H}_{11}\text{N}_7\text{OS}$: Calculated: C, 51.68; H, 3.41; N, 30.14; Found: C, 51.66; H, 3.40; N, 30.18.

4.2.1.14. 2-(4-(1H-tetrazol-5-yl)-1H-pyrazol-1-yl)-4-(3-methoxyphenyl)thiazole. (6n)

Green-crystals; Yield: 69%; M.p: 241-243 °C; MW: 325.35; R_f : 0.63; FT-IR (ν_{max} ; cm^{-1} KBr): 3487 (N-H stretch), 3072, 2974 (C-H stretch), 1678 (C=N stretch), 1670 (C-O stretch), 1261 (C-N stretch),

1182 (C-S), 787, 685 (C-S-C) cm^{-1} ; $^1\text{H-NMR}$ (400MHz, CDCl_3 , TMS) δ ppm: 8.96 (d, 1H $J=1.89$ Hz, pyrazol), 8.18 (s, 1H thiazole), 8.18 (d, 1H $J=1.47$ Hz, pyrazol), 7.47–7.44 (m, 2H, Ar-H), 7.01–6.98 (m, 2H, Ar-H), 3.67 (s, 3H, OCH_3), 3.53 (br-s, 1H, tetrazol, NH); $^{13}\text{C-NMR}$ (100MHz, CDCl_3) δ , ppm: 163.7, 161.1, 158.4, 149.2, 137.6, 134.2, 130.4, 129.3, 119.8, 114.3, 113.6, 108.5, 102.3, 55.2; Mass: 326.34 (M+1); Elemental analysis for $\text{C}_{14}\text{H}_{11}\text{N}_7\text{OS}$: Calculated: C, 51.68; H, 3.41; N, 30.14; Found: C, 51.64; H, 3.40; N, 30.16.

4.1.2.15. 2-(4-(1H-tetrazol-5-yl)-1H-pyrazol-1-yl)-4-(2-methoxyphenyl)thiazole. (6o)

Green yellow-crystals; Yield: 81%; M.p: 233-235 °C; MW: 325.35; R_f : 0.61; FT-IR (ν_{max} ; cm^{-1} KBr): 3492 (N-H stretch), 3079, 2971 (C-H stretch), 1682 (C=N stretch), 1679 (C-O stretch), 1268 (C-N stretch), 1187 (C-S), 781, 683 (C-S-C) cm^{-1} ; $^1\text{H-NMR}$ (400MHz, CDCl_3 , TMS) δ ppm: 8.93 (d, 1H $J=1.85$ Hz, pyrazol), 8.23 (s, 1H thiazole), 8.17 (d, 1H $J=1.57$ Hz, pyrazol), 7.55–7.52 (m, 2H, Ar-H), 7.01–6.97 (m, 2H, Ar-H), 3.78 (s, 3H, OCH_3), 3.52 (br-s, 1H, tetrazol, NH); $^{13}\text{C-NMR}$ (100MHz, CDCl_3) δ , ppm: 163.6, 158.5, 157.3, 152.7, 137.6, 131.1, 129.7, 129.2, 121.5, 118.9, 111.6, 108.5, 102.3, 56.1; Mass: 326.37 (M+1); Elemental analysis for $\text{C}_{14}\text{H}_{11}\text{N}_7\text{OS}$: Calculated: C, 51.68; H, 3.41; N, 30.14; Found: C, 51.67; H, 3.39; N, 30.15.

4.2. Assessment of PDE3A and PDE3B inhibitory activity

Assays were conducted following the instruction from the manufacture of the assay kit. The enzymatic reactions were conducted at room temperature for 60 min in a 50 μl mixture containing IMAP Reaction Buffer, 100 nM FAM-cAMP, 1 ng PDE3A or PDE3B and the test compound. The binding reactions were performed in the present of Binding Reagent (1:600 dilution in a reagent binding buffer containing 85% Binding Buffer A and 15% Binding Buffer B) at room temperature for 60 min. Fluorescence intensity was measured at an excitation of 485 nm and an emission of 528 nm using a BioTek Synergy™ 2 microplate reader. PDE3 activity assays were performed in duplicates at each concentration. Fluorescence intensity is converted to fluorescence polarization using the Gen5 software. The fluorescence polarization data were analyzed using the computer software, Graphpad Prism. The highest value of fluorescence polarization (FP_t) in each data set was defined as 100% activity. In the absence of PDE3, the value of fluorescent polarization (FP_b) in each data set was defined as 0% activity. The percent activity in the presence of the compound was calculated according to the following equation: %binding = $(\text{FP} - \text{FP}_b) / (\text{FP}_t - \text{FP}_b) \times 100$, where FP = the fluorescence polarization in the presence of the compound, FP_b = the fluorescent polarization in the absence of PDE3, and FP_t = the highest fluorescent polarization in each data set. The IC_{50} values were determined from the % activity of the enzymes at 0.01, 0.1, 1, 10 and 100 μM concentrations of synthetic inhibitors using sigmoidal dose–response curve in Graphpad Prism.

4.3. Assessment of inotropic and chronotropic activities

The whole atrium was separated from ventricle (for each compounds six atrium was used) and mounted vertically in a 50 ml organ-bath containing Krebs–Henseleit solution constantly gassed by 95% O_2 and 5% CO_2 , 35–37 °C, pH of 7.35–7.45. The bathing solution was made up (in mM): NaCl 118, KCl 4.5, CaCl_2 1.36, MgSO_4 1.21, NaH_2PO_4 1.22, NaHCO_3 25, and glucose 11.

Resting tension was adjusted to about 0.5 g in the whole atria and the initial equilibration period was 40–50 min for each preparation. Since the atria were isolated from reserpine-pretreated animals, depletion of catecholamines was verified by lack of any positive inotropic effect induced by tyramine (1.5 μM). Experiments were performed only in preparations that did not response to tyramine. The test compounds were added cumulatively (1–100 μM) and the responses of each concentration were recorded up to the maximum.

4.4. Sub-acute oral toxicity of compound 6d

In view of potent cardiotoxic activity of 6d in in-vitro model, sub-acute oral toxicity of the same was carried out in Swiss albino mice for its further development as viable drug candidate. Acute toxicity test has been completed and found that compound has been found to be safe upto 1000 mg/kg as a single acute oral dose. Hence, sub acute experiment was conducted in the present study in accordance with the Organization for Economic Co-operation and Development (OECD) test guideline No 423 (1987).

For the sub-acute oral toxicity study, 30 mice (15 male and 15 female) were taken and divided into five groups comprising 3 male and 3 female mice in each group weighing between 20 and 25 g. The animals were maintained at 22 ± 5 °C with humidity control and also on an automatic dark and light cycle of 12 h. The animals were fed with the standard mice feed and provided ad libitum drinking water. Mice of group 1 were kept as control and animals of groups 2, 3, 4 and 5 were kept as experimental. The animals were acclimatized for 7 days in the experimental environment prior to the actual experimentation. The test compound was solubilized in dimethyl sulphoxide and then suspended in caboxymethyl cellulose (CMC, 0.7%) and was given at 0.1, 1, 10 and 100 mg/kg body weight to animals of groups 2, 3, 4 and 5 respectively once orally for 28 days. Control animals received only vehicle.

References

- Smith, S. C.; Collins, A.; Ferrari, R. *J. Am. Coll. Cardiol.* **2012**, *60*, 2343.
- WHO Fact Sheet, Cardiovascular Diseases (CVD), World Health Organisations, N°317, Updated January 2015 (assessed on 13/03/15).
- Mathers, C. D.; A. Lopez, C.; Stein, D.; Ma Fat, C.; Rao, M.; Inoue, and others. 2001. "Deaths and Disease Burden by Cause: Global Burden of Disease Estimates for 2001 by World Bank Country Groups." In *Disease Control Priorities Project Working Paper 18*. Bethesda, MD.
- Lopez, AD. *World Health Stat Q.* **1993**, *46*, 91–96.
- Go, A. S.; Mozaffarian, D.; Roger, V. L.; Benjamin, E. J.; Berry, J. D.; Borden, W. B.; Bravata, D. M.; Dai, S.; Ford, E. S.; Fox, C. S.; Franco, S.; Fullerton, H. J.; Gillespie, C.; Hailpern, S. M.; Heit, J. A.; Howard, V. J.; Huffman, M. D.; Kissela, B. M.; Kittner, S. J.; Lackland, D. T.; Lichtman, J. H.; Lisabeth, L. D.; Magid, D.; Marcus, G. M.; Marelli, A.; Matchar, D. B.; McGuire, D. K.; Mohler, E. R.; Moy, C. S.; Mussolino, M. E.; Nichol, G.; Paynter, N. P.; Schreiner, P. J.; Sorlie, P. D.; Stein, J.; Turan, T. N.; Virani, S. S.; Wong, N. D.; Woo, D.; Turner, M. B.; American Heart Association Statistics Committee and Stroke Statistics Subcommittee. *Circulation* **2013**, *127*, e6–e245.
- Gaziano T. A. *Circulation.* **2005**, *112*, 3547–3553.
- Mason, D. T.; Foerster, J. M. Side Effects and Intoxication of Cardiac Glycosides: Manifestations and Treatment, In *Cardiac Glycosides Handbook of Experimental Pharmacology*, 1981, Volume 56 / 2, pp 275-297.
- Hauptman, P. J.; Kelly, R. A. *Circulation* **1999**, *99*, 1265-1270.
- Sutherland, E. W. *J. Biol. Chem.* **1958**, *232*, 1077–1091.
- Bender, A. T.; Beavo, J. A. *Pharmacological Reviews* **2006**, *58*, 488-520

11. Boswell-Smith, V.; Spina, D.; Page, C. P. *British J. Pharm.* **2006**, *147*, S252–S257.
12. Ramos Martins, D.; Pazini, F.; de Medeiros Alves, V.; Santana de Moura, S.; Morais Lião, L.; Torquato Quezado de Magalhães, M.; Campos Valadares, M.; Horta Andrade, C.; Menegatti, R.; Lavorenti Rocha, M. *Chem Pharm Bull (Tokyo)*. **2013**, *61*, 524-31.
13. Finar, I. L.; Godfrey, K. E. *J. Chem. Soc.* **1954**, 2293–2298.
14. Johansson, A.; Abrahamsson, M.; Magnuson, A.; Huang, P.; Mårtensson, J.; Styring, S.; Hammarström, L.; Sun, L.; Akermark, B. *Inorg. Chem.* **2003**, *42*, 7502–7511.
15. Lalehzari, A.; Desper, J.; Levy, C. J. *Inorg. Chem.* **2008**, *47*, 1120–1126.
16. Ballini, R.; Fiorini, D.; Palmieri, A. L. *Synlett* **2003**, *12*, 1841–1843.
17. <http://www.ncbi.nlm.nih.gov/BLAST/Blast.cgi>.
18. Altschul, S. F.; Madden, T. L.; Schäffer, A. A.; Zhang, J.; Zhang, Z.; Miller, W.; Lipman, D. J. *Nucleic Acids Res.* **1997**, *25*, 3389–3402.
19. Schäffer, A. A.; Aravind, L.; Madden, T. L.; Shavirin, S.; Spouge, J. L.; Wolf, Y. I.; Koonin, E. V.; Altschul, S. F. *Nucleic Acids Res.* **2001**, *29*, 2994–3005.
20. Sadeghian, H.; Seyedi, S. M.; Saberi, M. R.; Shafiee Nick, R.; Hosseini, A.; Bakavoli, M.; Mansouri, S. M. T.; Parsaee, H. J. *Enzyme Inhib. Med. Chem.* **2009**, *24*, 918–929.
21. Wu, G., Robertson, D. H., Brooks, C. L. and Vieth, M. *J. Comput. Chem.*, **2003**, *24*, 1549–1562. Ling, R.; Yoshida, M.; Mariano, P. *S. J. Org. Chem.* **1996**, *61*, 4439–4449.
22. Goering, B. K. Ph.D. Dissertation, Cornell University, 1995.
23. Haslam, E. *Shikimic Acid Metabolism and Metabolites*, John Wiley & Sons: New York, 1993.
24. Buchanan, J. G.; Sable, H. Z. In *Selective Organic Transformations*; Thyagarajan, B. S., Ed.; Wiley-Interscience: New York, 1972; Vol. 2, pp 1–95.
25. Lyle, F. R. U.S. Patent 5 973 257, 1985; *Chem. Abstr.* **1985**, *65*, 2870.

Research Highlight

- Compound 6d exhibited most potent inhibition of PDE3A than PDE3B.
- It buried deep inside the PDE pocket lined with residues like Tyr737, Phe559 and Phe991.
- It shows no observational changes, morbidity and mortality in experimental animals in toxicity assay

Graphical

